

Multi-methodological Characterisation of Medieval to Early Modern Coral Beads from a Cesspit of the “Fronerei auf dem Schranken” in Lübeck (Germany)

K. Bente, C. Berthold, R. Wirth, A. Schreiber and A. König

Keywords

Coral artefacts, Hanseatic Age, Lübeck, multimethodic archaeometry

Abstract

Eight late medieval to early modern red beads representative of a total of 41 from a cesspit of the “Fronerei auf dem Schranken” in Lübeck, Germany, were investigated using micro X-ray computed tomography (3D- μ XCT), X-ray microdiffraction (μ -XRD²), transmission electron microscopy (HRTEM) and Raman spectroscopy (RS). The microscopic properties of the material were characterised non-destructively or minimally invasively for colouration, mineralogical and chemical composition determination but also with regard to their macroscopic external appearance. The polished beads are spherical with flattered tops and boreholes perpendicular to the flattening and show partially traces of working. As base material for all examined beads, high Mg-Calcite with polyenes could be identified. Combined with density and microstructure data, the beads are undoubtedly red precious corals, identical with modern *corallium rubrum* from the Mediterranean also confirmed by C- and O-isotopic analyses. The studies provide general criteria for the determination of *corallium rubrum*, confirming the macroscopically determined identification of other coral artefacts associated with the Hanseatic League, and thus prove their iconographic importance as well as the trade contacts with the Mediterranean region. However, the extent to which the characteristics of the coral beads indicate accidental or intentional individual or collective societal or social circumstances is left to further study.

Introduction

Corals as ritual objects and jewellery can be regarded as quite typical in Hanseatic societies. The raw material derives from the Mediterranean Sea sourced in particular

from Italy (Schrickel, et al., 2014; Schrickel and Bente, 2013; Fürst, 2014). Reaching norther parts of Europe via trading posts and middlemen (Esser, 1898; Volckmann, 1921; Ritz, 1975) the coral became increasingly precious. Until today, the raw coral materials (Filip, 1969; Schumann, 1976) are processed using saws, files, drills and polishing agents. Spherical coral beads and rollers or cylinders often show the former branch structure of the raw material, which, however, does not appear on the beads examined here. Since corals were very expensive and valuable, imitations are often found as so-called “fake corals” made of very different and even artificially coloured materials (Grimm and Grimm, 1971). In popular belief (Grabner, 1969), the importance of corals was linked to its strong counterforces against mental and physical unhappiness as well as against the evil eye, melancholy and various diseases, and also against storms and witchcraft (Daxelmüller, 1982). They should also promote “joie de vivre” (Wittstock, 1981; Brückner, 1970). Thus, in the late medieval Ages, necklaces of cut “corals” as jewellery and painted within pictures (Legner, 1978; Hasse, 1961, 1981a, 1981b) are often found. Besides amber (Falk, 1987; Hasse, 1961; 1981a; 1981b; Esser, 1898; Fritz, 1982), coral was the predominant material for rosaries (Grimm and Grimm, 1971; Erdmann, 1985a; 1985b; Erdmann and Nitsch, 1986; Hasse, 1981a), which, combined with the brotherhood system (Hauschild, 1981), reached its peak in the second half of the 15th century until the Reformation.

Red artefacts either as single precious objects or as decorative elements from different periods are mostly thought to derive from *corallium rubrum* because of their colour (Schrickel, 2014), context and shape. Their main material significance is defined by polyenes as the red pigment (Urmos, Sharma and Mackenzie, 1991), high Mg contents of the calcites (Han, et al., 2013) and the

microstructure of the biogene calcites showing typical meso-crystallinity (Floquet, et al., 2015; Vielzeuf, et al., 2008; Fan, 2018). Surface phenomena of original *corallium rubrum* like linear grooves often found on e.g. Iron Age coral artefacts (Bente, et al., 2021a) and described as identification criteria (Fürst, 2014), are not detected on beads described here because they are processed by forming and polishing. Because red coralline material is often substituted by other and cheaper red materials such as glass, enamel, amber, ceramics etc. (Grimm and Grimm, 1971; Bente, et al., 2015), the artefact materials have to be determined conclusively. This requires multi-methodological approaches for a comprehensive chemical and structural characterisation. As also reported by Fürst (2014) for Iron Age coral jewellery, it is necessary to carry out comparative studies on artefacts from different times, regions and cultures, which are classified by appearance as corals, as well as on recent precious coral, *corallium rubrum*. However, in contrast to original coral morphologies showing e.g. typical grooves, polished bead do not show such significant macroscopic characteristics and have therefore to be analysed due to their volume properties. The results then are used for archaeological interpretations e.g. origin, trade routes, quality of craftsmanship and traces of processing as well as secondary alteration of the materials. The results are compared to data of *corallium rubrum*. The results implying isotopic data (Bente, et al., 2021b) will be discussed related to coral beads from Greifswald (Bente, et al., 2017) and original *corallium rubrum* (Chaabane, et al., 2015). The results could also be used for a better understanding of white coral decorations of Iron Age jewellery (Fürst, 2014; Keuper, et al., 2015).

Artefacts

Provenance of the coral artefacts

The coral beads under investigation were provided by the agency of preservation of archaeological monuments of the city of Lübeck. The artefacts were discovered in 1976 during excavations “auf dem Schranken” in Lübeck by the University of Kiel together with the Office for Pre- and Early History (preservation of archaeological monuments) of the Hanseatic City of Lübeck. The artefacts were excavated in the southern wing of the *Fronerei*, the residential and official building of the *Fronen* (Herrmann, 1986; Erdmann, 1980; 1985a; 1985b). As in many other settlements e.g. the Hanseatic city of Greifswald (Bente, et al., 2017), cesspits are often used as garbage pits by temperously different social groups and

within different parts of buildings. In the cesspit of the *Fronerei* 139 single beads of different material such as wood, amber, bone, agate were found, and especially 41 single coral beads and a completely preserved coral bead necklace with a prominent phallic bead and two further bead necklaces. Comparatively valuable finds were only observed in lower, but not in the upper cesspit layers from the second half or the last third of the 15th century (Hammel, 1987). The coral materials from the different find heights were therefore divided into two temporally different groups, resulting from the partial emptying around 1450/60 and refilling of the cesspit presumably in the last third of the 15th and first half of the 16th century.

Description of the artefacts

The artefacts analysed in this work are single beads found next to a necklace with a phallic bead in the cesspit of the “Fronerei auf dem Schranken” at Lübeck (Erdmann, 1985a; 1985b). Wehrmann (1984), Stephan (1978) and Mührenberg (1984) discuss the dating of these finds. However, these single beads and also necklace beads should reflect individual circumstances of the households or fronts (Erdmann, 1985a; 1985b), which can also be related to the decrease or absence of coral beads in the younger cesspit layers of the 15th century (Wittstock, 1981). The eight read beads (Figure 1) analysed in this study were selected from a total of 41 late medieval to early modern beads. One bead (HL_2_301) shows superficial small whitish areas (Figure 1). The beads macroscopically identified to be coral makes up approx. 27 % of the single beads (excluding necklaces/rosaries – Pater Noster), and this is because of the 41 beads found at height of 6.00-6.50 m above sea level, lying close together, but not necessarily being a single string of beads. The beads are salmon-red, cylindrical oval and flattened to about 1/3, while pure spherical beads are missing. The sizes of the beads vary slightly and are quite uniform in shape. The eight beads examined have outer diameters of 4.5 mm to 6.2 mm and a drill hole of ca. 1.5 mm slightly changing. Their height is typically about three quarters of the outer diameter. The barrel-shaped beads imitate the original branch shape of coral skeletons, while the coral artefacts from Greifswald (Bente, et al., 2017) are somewhat flatter. The coral beads from Lübeck are shown in Figure 1.

Methods

In order to determine the material as well as general properties of coral artefacts, the coral beads from Lübeck

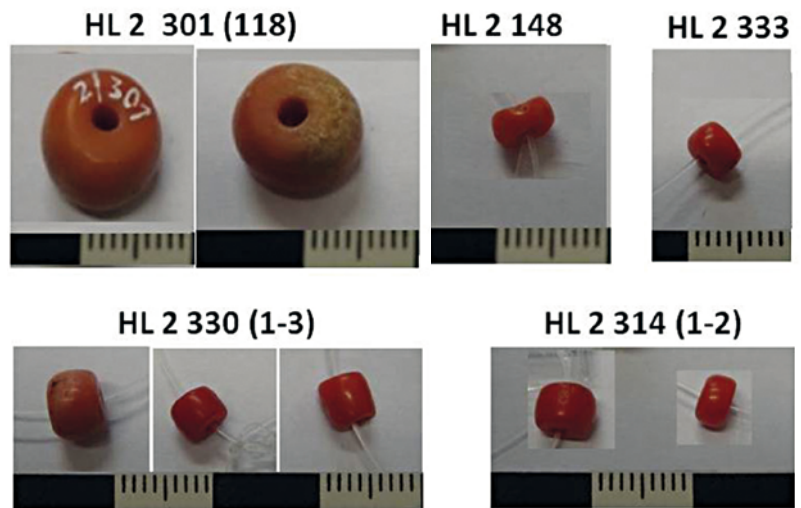


Figure 1. Photos of the eight examined coral beads. HL_2_301 upper and lower surface and parts that appear superficially white in some places, all other beads are shown with only one photo each. Photo: K. Bente.

were studied due to their chemical composition (organic matrix, red polyene dye), biomineral calcite properties (MgCO_3 content in $\text{Mg}_x\text{Ca}_{1-x}\text{CO}_3$) and microstructure (density, pores, defects). Non-destructive (μXCT , XRD and Raman spectroscopy) methods and minimally invasive (TEM) methods were used and are described below. While Raman spectroscopic and XRD data were systematically collected for all beads CT studies were performed for 3 representative beads. Based on these data additional TEM studies were performed on different parts of one exemplary bead using electron diffraction, HRTEM and AEM.

1. Micro x-ray computer tomography (μXCT):

μXCT was used for non-destructive 3D imaging of the inner structure of coral objects and e.g. inside relic structures and cavities. (Bente, et al., 2017). The investigations were carried out by means of W-radiation in reflection with 160 kV, 130 μA , 0.1 and 0.5 mm Cu-filter at 1600 projections and a square flat panel detector (2028^2 pixels, pitch size $200^2 \mu\text{m}$) and a resolution of 7- 10 μm voxel edge. The 2D and 3D images are displayed inversely with respect to the grey values, so that higher absorptions correspond to lighter greys.

2. X-ray diffraction (XRD):

Typically, metastable biogenic coral calcites, which are formed in seawater, are characterised as so-called “High Magnesium Calcite (HMC)” by MgCO_3 contents $> 7 \text{ mol } \%$ (Railsback, 2006). The incorporation of Mg-cation in the calcite lattice results in a decrease of the lattice constants. Therefore correlated with chemical reference data, the Mg content of calcite can be determined using X-ray diffraction by the position of the 104-calcite main peak, which was shown for inorganic Mg-Calcites in the 60th by Goldsmith (1961) and later

also for biogenic Mg-Calcites by e.g. Han, et al. (2013). The X-ray diffractometer measurements were performed non-destructively with a Bruker D8-discover microdiffractometer equipped with a Co X-ray tube running at 30kV/30mA, a graphite primary monochromator, X-ray optics with 300 μm beam diameter and a large two-dimensional VANTEC 500 detector ($\mu\text{-XRD}^2$). Beside the angular resolution of the instrument of $0.05^\circ 2\text{Theta}$ the uncertainty in peak position is app. $0.1^\circ 2\text{Theta}$ caused by the surface topology resulting in an absolute error of 2 % in the Mg-content (mol % MgCO_3 in $\text{Mg}_x\text{Ca}_{1-x}\text{CO}_3$). In order to check Mg contents at different areas of one bead, Mg content data were calculated using d_{104} reflection. At the University of Leipzig, a Bruker D8 Discover microdiffractometer equipped with a CuK α ($\lambda = 1.5418 \text{ \AA}$) source, tube running 40.0 kV/40.0 mA, variable slit, beam diameter 1 – 4 mm² and a VANTEC-500 detector was used. For both data sets, a pure synthetic calcite from Merck was used as an external reference for instrumental calibration.

3. High-resolution transmission electron microscopy (HRTEM):

TEM studies with chemical analysis using analytical electron microscopy (AEM) were carried out using foils with dimensions of 1 μm produced by FIB (Focussed Ion Beam) milling. HRTEM allows the determination of microstructures with high resolution down to the nm range. High Angle Annular Dark Field (HAADF), Dark Field (DF) and Bright Field (BF) imaging were used to visualise the crystal and microstructures of the calcites and the organic matrix. Using AEM, the Mg contents of the calcites could be determined (mol % MgCO_3 in $\text{Mg}_x\text{Ca}_{1-x}\text{CO}_3$) with errors of 2 at %. The crystallinity of the calcites was determined by “selected area electron diffraction” (SAED). The instruments used at GFZ Potsdam

are FIB HELIOS G4 from Thermo Fisher (Ga ion source) and HRTEM TECHNAI G2 (200 kV) with field emission cathode from Thermo Fisher.

4. Raman spectroscopy (RS):

The organic red pigments i.e. polyenes (Urmos, Sharma and Mackenzie, 1991; Adar, 2017), which are typical for red corals, can be identified non-destructively by μ -Raman spectroscopy (Fürst, 2014; Keuper, et al., 2015; Bente, et al., 2015; 2017). The calculation of N_{eff} (Barnard and de Waal, 2006), representing the average number of C=C-bonding in the polyenes, cannot be deduced separately using the Raman bands but give at least information useful to compare the pigments. The Raman spectroscopic data were obtained with a μ -Raman spectrometer from Renishaw (InVia Reflex Raman Microscope) with a laser wavelength of 532 nm (green) with Rayleigh edge filter and measurements from 100 cm^{-1} to 1800 cm^{-1} or 2500 cm^{-1} . Selected comparative measurements e.g. at different sites of one bead were carried out at the University of Leipzig with XY-La-

ser-Raman-Spectrometer from Dilor with a laser wavelength of 514.5 nm.

Results

Micro X-ray computer tomography (μ XCT) studies

The μ XCT data of three exemplary beads are identical with data of authentic precious corals at resolutions of $\sim 10\ \mu\text{m}$, i.e. a dense material with few cavities showing diameters of $\sim 0.1\text{ mm}$ (Figures 2a-d). External morphologies and cavities can directly be related to μ XCT images. Later on, for characteristics within submicron dimensions, TEM studies were carried out.

XRD studies

The calcite composition (HMC) of the beads from the cesspit “auf dem Schragen” was examined by XRD measurements in order to check the Mg contents which

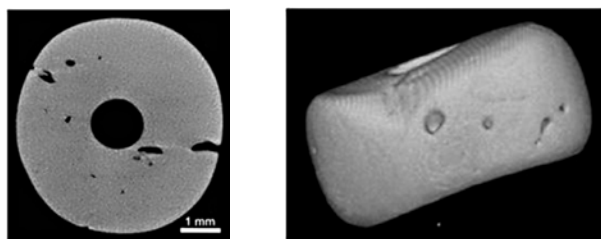


Figure 2a. μ XCT data of bead HL_2_148. Cross section with drill hole and volume voids (left) and a 3D projection (right) from a μ XCT measurement with different cavities opened during grinding and polishing. The ribbing/rippling visible on the top surface of the 3D-projection are artefacts from the CT-imaging process and do not represent the surface features (linear grooves) of the original coral skeleton.

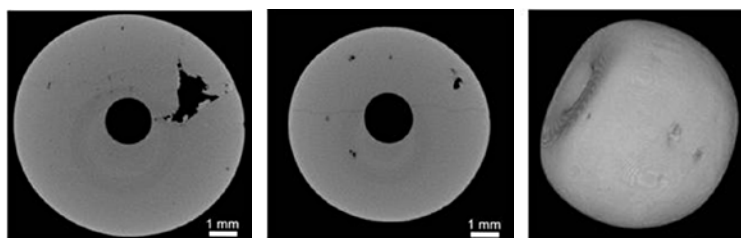


Figure 2b. μ XCT data Bead HL_2_301. Images of a measurement in two cross sections (left and centre) with drilling holes and differently sized cavities and on the right in a 3D projection with surface-exposed cavities. The ribbing feature of the 3D projection of the bead is an imaging effect as in Figure 2a.

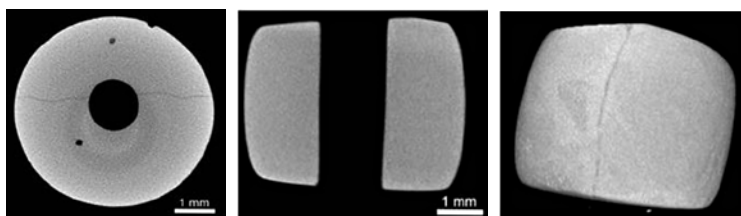


Figure 2c. μ XCT data of bead HL_2_330_1. Left: Two cracks starting from the drilling hole and continuing on both sides as well as an exposed cavity (top). Centre: 2D projection with drilling hole perpendicular to the left image. Right: 3D projection with crack appearing continuously on the surface, matching the crack on in left image.

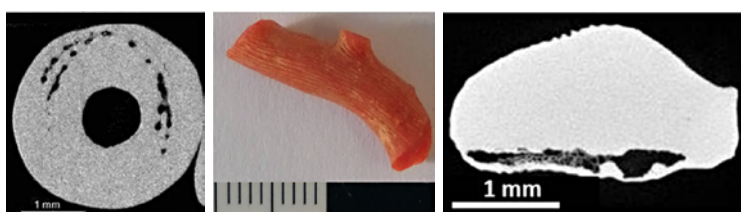
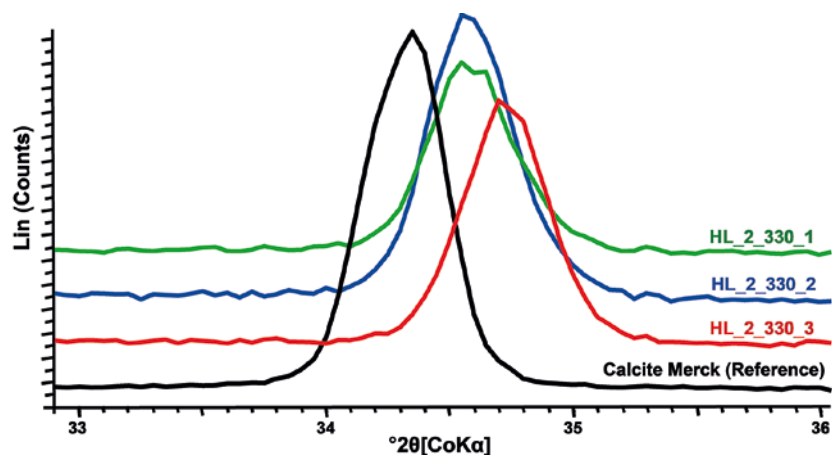


Figure 2d. μ XCT comparison measurements. Left: Bead 1 from Greifswald with concentric crack parallel to the cavity arrangement. Centre: Photo of an original *corallium rubrum* CR 4 with longitudinal grooves. Right: 2D μ XCT image (cross section) of CR 4 with tooth-like edges perpendicular to the longitudinal grooves as well as dense matrix and cavities similar to the cavities of a necklace bead from Greifswald (Bente, et al., 2017).

Photos: 2a-d: C. Berthold, R. Wirth, A. Schreiber and A. König; 2d centre: K. Bente.

Figure 3. Representative X-ray diffractograms (Co K α) showing the Position of the 104 intensity of three beads to illustrate the variation of the measured peak shift caused by the Mg cation in the Calcite lattice and reference pattern of the calcite standard (Merck).



are calculated from d104 (measured against a standard of Mg-free calcite from Merck) according to Goldsmith (1961). Typical X-ray diffractograms of selected beads with maximum and minimum Mg contents are shown together with the reference of a pure calcite (Merck) in Figure 3. The Mg contents estimated by the 104-peak position in mol % MgCO₃ with respect to Mg_xCa_{1-x}CO₃ are between app. 7 mol % and 11 mol % (+/- 2 %). For comparison, our measurements of modern *corallium rubrum* from the Mediterranean Sea show typical contents of MgCO₃ between 8.4 mol % and 8.7 mol % (+/- 2 %). These values of the Lübeck coral beads correspond to the Mg contents of the coral beads from Greifswald (Bente, et al., 2017). All Mg-contents were calculated from the 104-peak position referenced to the Mg-free Merck Calcite using the corresponding empirical correlations of Goldsmith (1961) and Han, et al. (2013), see Table 1.

HRTEM Studies

As the most significant example of the artefacts, the bead HL_2_301 was examined in comparison with different modern *corallium rubrum* branches of (CR 1, CR4, CR 5) from the Mediterranean Sea (provided by Ruppenthal company). In particular, HAADF, bright field and dark field images are used to determine the microstructure of the calcites and the organic matrix as well as the pore spaces and sizes, SAED to determine mesocrystallinity and AEM to determine growth-dependent Mg/Ca variations in calcite. Data from Perrin, et al. (2015) and Vielzeuf, et al. (2008), recorded on natural and synthetic *corallium rubrum*, are included. TEM data of bead 301 are recorded at an original red (HL_301_1 #6330) and at an area of white (HL_301-2 #6331) appearance. For comparison reasons TEM data of *corallium rubrum* (CR 4) are listed.

In Figure 4a and Figure 4b, the TEM data are presented for bead HL_2_301 with mesocrystals of high-

Table 1. Mg contents of all beads and two different *corallium rubrum* fragments calculated from the 2Theta values of the 104 intensity (Co K α radiation) using the correlation of natural corals from Goldsmith (1961) in accordance with synthetic HMC after Han, et al. (2013) in mol MgCO₃ with respect to Mg_xCa_{1-x}CO₃. *HL_2_301 with identical XRD data comparing the main red areas and a small whitish area, are both gained by using CoK α .

Bead No. / Recent <i>corallium rubrum</i>	MgCO ₃ mol % calculated from 104-peak
HL_2_148	9.5
HL_2_314-1	9.5
HL_2_314 2	7.4
HL_2_330-1	7.4
HL_2_330-2	7.4
HL_2_330-3	10.6
HL_2_333	8.5
HL_2_301 red area	6.8
HL_2_301 white area	6.8
CR 4 <i>corallium rubrum</i>	8.4
KO-1 <i>corallium rubrum</i>	8.8
*HL_2_301 red & white	6.8

Mg calcite (HMC), and the corresponding diffraction images and AEM data indicate growth-related variations in the Mg contents of the calcites (HMC). These data are compared with the data (Figure 5) of an original *corallium rubrum* branch (CR 4). The Mg contents are given in mol % MgCO₃ in Mg_xCa_{1-x}CO₃. These electron microscopic images of the white areas of bead HL_2_301 (Figure 1) show a lamellar arrangement of HMC mesocrystals typical for *corallium rubrum* in bright field imaging (Figure 4a, Figure 4b). The red areas differ from the superficial white areas only in that the white areas have relatively more and larger cavities (Figure 4c).

Comparative TEM measurements of *corallium rubrum* and red beads from Lübeck also show identi-

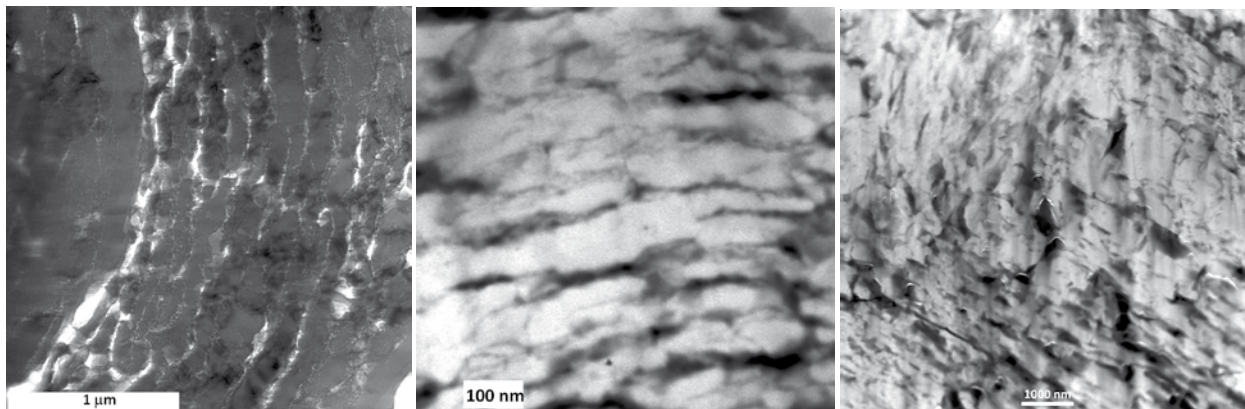


Figure 4a. Left: Bright-field image of a red coloured area with annular microstructure of the arrangement of mesocrystals within organic matrix of the bead HL_2_301- white areas represent porosity. Photo: C. Bente.

Figure 4b. Middle: HAADF image of a red coloured area of lamellar mesocrystal arrangements (bright) and organic matrix but also cavities (black), which could not be differentiated of the bead HL_2_301. Photo: C. Bente.

Figure 4c. Right: HAADF image of the whitish area of the bead HL_2_301 (#6331) with significantly larger number and dimensions of cavities relative to red coloured areas. In the HAADF images, pores are shown with dark contrast. Photo: C. Bente.

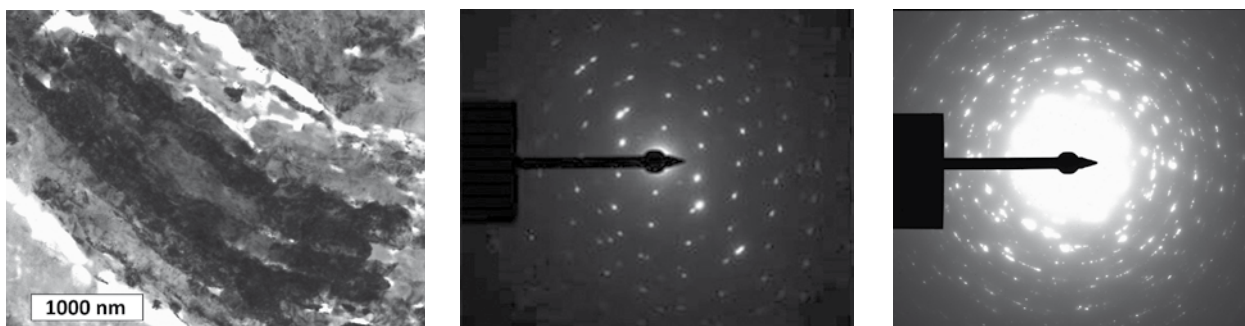


Figure 4d. Left: Bright filed (BF) image of a mesocrystal selected from BF image in Figure 4a of HL_2_301 with typical diffraction contrast for a mesocrystal identical with the bright field image of *corallium rubrum* in Figure 5. Photo: C. Bente.

Figure 4e. Middle: Electron diffraction of one mesocrystal from Figure 4d with elongated peaks. Photo: C. Bente.

Figure 4f. Right: Electron diffraction of several mesocrystals of the selected bead HL_2_301 (complete mesocrystal arrangement in Figure 4b). Photo: C. Bente.

cal high-resolution images and diffraction patterns of mesocrystalline HMC and, based on AEM data, comparable Mg contents of ~ 7-10 mol % MgCO₃.

The selected MgCO₃ contents recorded by AEM are listed in Table 2 using the red and white areas of the bead HL_2_301 together with AEM comparison data of two modern *corallium rubrum* (CR 5, CR 1).

The electron diffraction images of individual mesocrystals (Figure 4d) of both areas show slightly broadened and multiple reflections (Figure 4e), whereas single crystals show ideally point like reflections: This corresponds to the arrangement of nanocrystals that are also only slightly tilted against each other, which is also reported in the literature (Floquet and Vielzeuf,

Table 2. Selected locally high-resolved MgCO₃ contents by AEM in mol % with corresponding measurement (errors of 2 %) of white and red regions of the representative bead HL_2_301 compared with two modern *corallium rubrum* CR 1 and CR 5.

Bead HL_2_301; <i>Corallium rubrum</i>	MgCO ₃ mol % Position 1	MgCO ₃ mol % Position 2	MgCO ₃ mol % Position 3	MgCO ₃ mol % Position 4
HL_2_301 red	7.4	8.8	9.1	10.1
HL_2_301 white	5.1	6.2	6.7	10.0
CR 5 <i>corallium rubrum</i>	7.1	8.8	9.1	9.9
CR 1 <i>corallium rubrum</i>	5.4	6.5	6.5	7.0

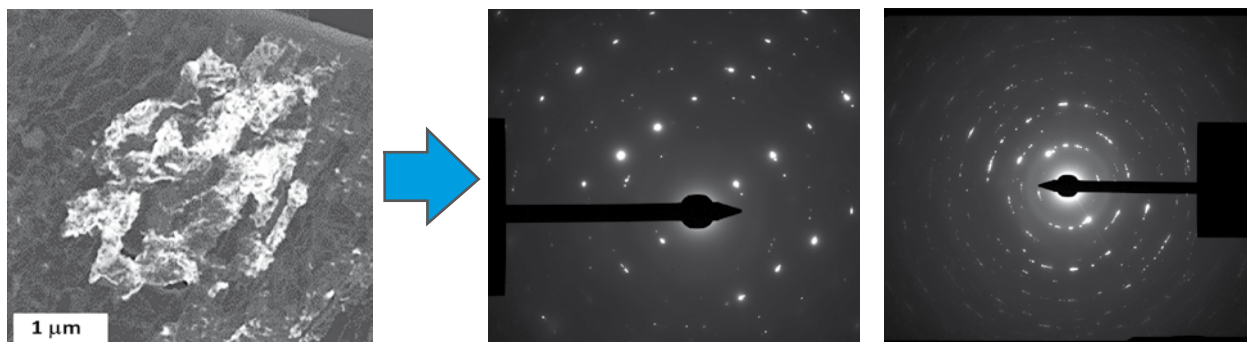


Figure 5. Original *corallium rubrum* CR 4 (#6243). Left: Bright field image of a mesocrystal of about 3 μm length in the middle of the image with diffraction contrast identical with BF of HL_2_301 in Figure 4d. Middle: SAED of a single mesocrystal (central area from Figure 5 with typical elongated peaks). Right: SAD of multi-mesocrystal arrangement in CR 4 identical with the arrangement in HL_2_301 Figure 4b and its SAD in Figure 4f with overlapping pattern. The corresponding local Mg contents (AEM) due to the growth conditions are between 7 and 9 mol % MgCO_3 with a measuring error of 2 %. Photo: C. Bente.

2011; Fan, 2018). Electron diffraction images of several mesocrystals, which are more strongly tilted against each other, accordingly show superimposed reflex patterns (Figure 4f) of the involved mesocrystals, which are in agreement with the mesocrystals of *corallium rubrum* (Figure 5). The lengths of the mesocrystals are between 3.0 and 4.0 μm . The Mg contents of the HMC for the white and the red region of bead HL_2_301 were determined by AEM between ~ 5 and 10 mol % MgCO_3 with errors of ~ 2.5 %. The red parts of the bead HL_2_301 (#6330) show typical mesocrystalline areas within embedded organic matrix and relatively few cavities. In contrast, the few patchy white areas of bead HL_2_301 (#6331) show some more and relatively larger cavities.

These electron microscopic results of the red regions of bead HL_2_301 are identical with the TEM data of original *corallium rubrum* as shown for sample CR 4 in Figure 4b. Due to the agreement of the locally highly resolved Mg contents of the bead HL_2_301 with *corallium rubrum* (CR 1, CR 5) between 5 and 10 mol % MgCO_3 using AEM, the diagnostic criteria of the coral characteristics of the artefacts are confirmed. The variable Mg contents in an object correspond to the growth conditions, which are consistent with the average XRD data.

Raman spectroscopic studies

The selected beads, if they contain polyenes, should show the typical red-coloured Raman bands of *corallium rubrum* in the range of at $\nu_2 = \sim 1128 \text{ cm}^{-1}$ and $\nu_1 = \sim 1518 \text{ cm}^{-1}$ (Karampelas, et al., 2009). In such polyene mixtures C=C stretching modes at $\sim 1530 \text{ cm}^{-1}$ are present, from which the effective number of C=C bonds can

be calculated using the approach of Barnard and de Waal (2006). While the polyenes (parrodiene) typical for the coral skeleton are non-methylated polyacetylenes, which show C-C stretching modes 2 at $\sim 1130 \text{ cm}^{-1}$, methylated polyacetylenes (carotenoids) are characterised by 2 values around 1160 cm^{-1} (Fritsch, et al., 2009). The band positions of the polyenes of the beads from Lübeck with measurements at $\lambda = 514 \text{ nm}$ (Dilor) and $\lambda = 532 \text{ nm}$ (Renishaw) are listed together with reference materials in Table 3 as well as graphically represented with examples from bead HL_2_330 (white and red spot) in Figure 6a and 6b. The data are identical within the margins of error. The individual polyenes with different numbers of C=C bonds present in the polyene mixtures in different proportions cause a shift of the bands (Kupka, et al., 2010). The referenced band positions of the measurements are used for the calculation of N_{eff} (Barnard and de Waal, 2006) in order to characterise the polyene mixture characteristics.

The results of Raman spectroscopy ($\lambda = 532 \text{ nm}$) of the beads HL_2_301, HL_2_314, HL_2_148, HL_2_330, HL_2_333) with typical polyene bands at $\nu_2 = 1128 \text{ cm}^{-1}$ and $\nu_1 = 1516 \text{ cm}^{-1}$, while spectra of natural *corallium rubrum* (CR 4, KO-1) were recorded at $\lambda = 514 \text{ nm}$ (Table 3). Additionally, for reasons of comparison, data of red African Ethnographica (Bente, et al., 2015) and white *corallium rubrum* artefacts from Bad Dürrenberg (Keuper, et al., 2015) are also listed. The measured values of the bands for the beads from Lübeck are identical at the respective wavelengths within the margins of error. The bands at the white and red points of bead HL_2_301 and HL_2_330 do not differ either. Additionally the corresponding XRD data of the Mg-content are also identical. The effective number of C=C double bonds (N_{eff}) according to Barnard and de

Table 3. Table of the corrected band positions for ν_1 and ν_2 ($\pm 0.5 \text{ cm}^{-1}$) of the beads from Lübeck including white and red spots, for 2 *corallium rubrum* (CR 4, KO-1) from the Mediterranean Sea, for a red bead from Greifswald (Mecklenburg-Vorpommern, Germany) and from African ethnographic red coral (Kingdom of Benin) as well as white beads from Bad Dürrenberg (Austria). The data of whitish and red parts, exemplarily shown for HL_2_330_1 and HL_2_330_2, are also identical. The effective number (N_{eff}) of C=C double bonds are also listed for all objects according to Barnard and de Waal (2006) and are approximately identical for the beads from Lübeck within the range of the errors (± 0.1).

Artefacts and <i>corallium rubrum</i>	$\nu_2 \text{ cm}^{-1}$ (± 0.5)	$\nu_1 \text{ cm}^{-1}$ (± 0.5)	$N_{\text{eff}} (\pm 0.1) =$ $e^{(1745 - \nu_1)/97.07}$
HL_2_148, HL_2_301, HL_2_314_1, HL_2_314_2, HL_2_301_1 red, HL_2_301_2 white	1128	1518	10.4
HL_2_330_1, HL_2_330_2, HL_2_330_3	1129	1516	10.6
HL_2_333	1128	1518	10.4
<i>Corallium rubrum</i> : CR 4 light red, CR 4 dark red, KO-1	1126.5	1517	10.5
Red beads Greifswald	1132	1521	10.0
African Ethnographica Red coral inlay	1130	1519	10.3
White Fibula inlay (Bad Dürrenberg, Austria)	1133	1525	9.6

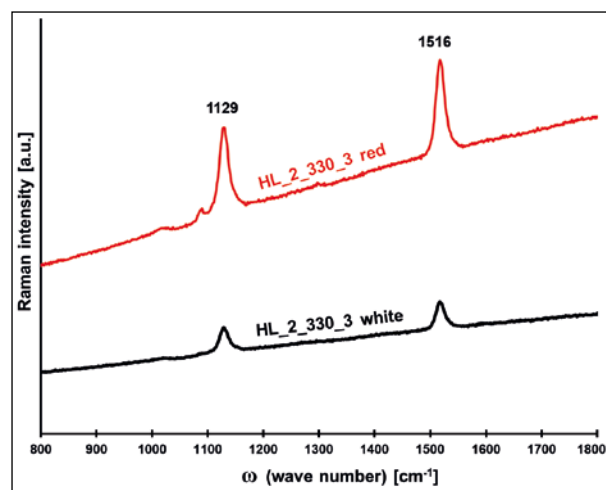


Figure 6a. Raman spectra by laser of $\lambda = 532 \text{ nm}$ of the bead HL_2_330_3. Red and white areas (Figure 1) without difference of the typical polyene bands for C-C stretching mode at $\nu_2 = 1129 \text{ cm}^{-1}$ and for C=C stretching mode at $\nu_1 = 1516 \text{ cm}^{-1}$ (Table 3).

Waal (2006) results in $10.4 < N_{\text{eff}} < 10.6$ for the beads from Lübeck as well as $N_{\text{eff}} = 10.0$ for a red comparison bead from Greifswald, $N_{\text{eff}} = 10.3$ for another red beads from the Kingdom of Benin (~ 1800) and $N_{\text{eff}} = 9.6$ for an Iron Age white bead from Dürrenberg (Austria) (Keuper, et al., 2015). With decreasing N_{eff} , the number of polyenes with lower chain lengths in the respective polyene mixture increases, which corresponds to fewer C=C double bonds. The small bands at ca. 1090 cm^{-1} refer to calcite-magnesite mixed crystals (Clark, et al., 2010; Gunasekaran, Anblalagan and Pandi, 2006).

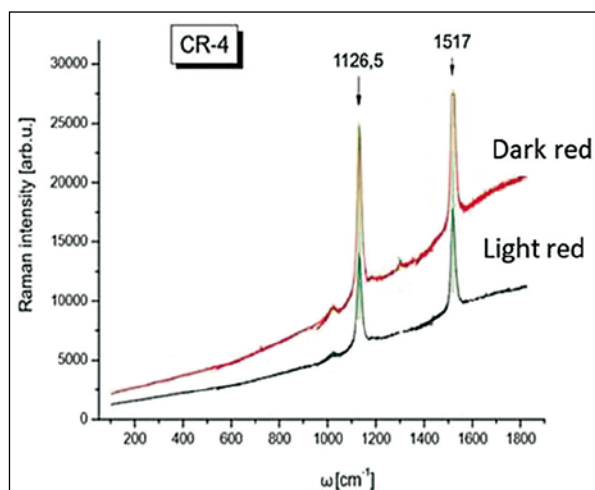


Figure 6b. Related Raman spectra by laser $\lambda = 514 \text{ nm}$ of an original *corallium rubrum* CR 4 from the Mediterranean Sea at a dark red and a light red spot: $\nu_2 = 1126.5 \text{ cm}^{-1}$ and $\nu_1 = 1517 \text{ cm}^{-1}$ (Table 3).

Conclusions and Outlook

Characterization of the beads

The beads were characterized using μXCT , XRD, HR-TEM, and Raman spectroscopy.

μXCT with its resolution of $7 - 10 \mu\text{m}$ showed that original corals and coral beads are relatively dense with cavities in the μm range. If those are opened during grinding and polishing they are visible as surface holes in μXCT images (Figure 2a-d). Two different crack

systems can be distinguished: concentric cracks can be assumed as primary phenomena of the raw corals, whereas the crack perpendicular to the borehole of bead HL_2_330_1 was probably caused by mechanical stress during drilling.

XRD data of the different beads show in all cases HMC with typical Mg contents of app. 7 – 11 mol % MgCO_3 in $\text{Mg}_x\text{Ca}_{1-x}\text{CO}$. Similar values were also reported for red coral beads of the Greifswald necklace (Bente, et al., 2017) and correspond to Mg contents of original red corals from the Mediterranean Sea, which suggests that *corallium rubrum* was the raw material in all cases. No difference could be found between the red and partly whitish surface parts of HL_2_301. White coral beads of Iron Age fibulae from Dürrenberg (Austria) and Langenau (Germany) show Mg contents in the same range (Schrickel, et al., 2014).

TEM analyses were carried out of red and whitish areas of bead HL_2_301 and different branches of modern *corallium rubrum*. Both materials show the typical 3.0 – 4.0 μm large mesocrystals with pores < 5 nm between and within the mesocrystals. Worth to be remarked that pore sizes around 40 nm (Bente, et al., 2021a; Peelen and Metselaar, 1974) only occur in the small white surface area of bead HL_2_301. The Mg contents are determined with AEM corresponding to the data obtained by X-ray diffraction.

Raman spectra of all investigated beads and original corals show bands at $\nu_2 = 1128 - 1130 \text{ cm}^{-1}$ and $\nu_1 = 1516 - 1521 \text{ cm}^{-1}$, which are typical for pink and red corals (Hedegaard, Bardeau and Chateigner, 2006; Urmos, Sharma and Mackenzie, 1991; Karampelas, et al., 2009; Kupka, et al., 2010; 2016a; 2016b; Fan, 2018). The N_{eff} of the pigment polyenes ranging from 10.4 to 10.6 of the beads are in agreement with the data of *corallium rubrum*.

Archaeometric implications

The non-destructive and minimally invasive studies of the beads from the cesspit “auf dem Schranken” in Lübeck verify *corallium rubrum* from the Mediterranean Sea as raw material, comparable to other coral objects e.g. from Greifswald etc. These results are confirmed by actual isotopic data (Bente, et al., 2021b; Fohlmeister, et al., 2018) showing $\delta^{13}\text{C} = -0.29 \text{ ‰}$ and $\delta^{18}\text{O} = -0.13 \text{ ‰}$, which is in agreement with data of Adkins, et al. (2003) and Chaabane, et al. (2015). Identical with data of recent *corallium rubrum*, these data are typical for modern day sea water showing $15 < \text{B ppm} < 50$ and $10 \text{ ‰} < \delta^{11}\text{B} < 30 \text{ ‰}$ (Bente, et al., 2017). The presented multimethodical approach could be used in order to

establish identification criteria for red and white coral artefacts related to *corallium rubrum* as raw material. In addition, a detailed characterisation of the quality of grinding and polishing of such beads could also be taken in account in future in order to differentiate artisan skills.

Archaeological implications

Like the beads from Greifswald (Bente, et al., 2017), the beads of the Hanseatic League from Lübeck are undoubtedly made of red precious coral, *corallium rubrum*. They were turned, grinded and polished into balls, barrels and rollers as well as other shapes. The Lübeck beads and the approximately contemporaneous Greifswald beads have inner cavities exposed on the surface through grinding and polishing of the raw material. Furthermore, cracks found on one bead can be attributed to the mechanical stress during the production of the boreholes. In contrast to this, only concentric crack running parallel to natural cavity arrangements occur in the Greifswald beads. The raw materials or corresponding semi-finished products of the coral artefacts from Lübeck and the beads from Greifswald certainly derive from the Mediterranean area. In the era of the Hanseatic League, the corresponding trade is usually carried out through intermediaries. However, there are still open questions about the location of the processing of corals and by which may be other craft industries. To what extent the kind or quality of the processing of the coral beads points to coincidental individual or deliberately collective, i.e. social circumstances or fashions, cannot be determined based on a few studied artefacts. Further systematic studies are needed to establish generally valid criteria for red *corallium rubrum* artefacts and its whitened derivatives, as found in the Iron Age (Bente, et al., 2015; Schrickel and Bente, 2013).

Acknowledgement

Dr. M. Schneider and D. Mührenberg (Monument Protection Agency, Lübeck) provided the examined coral artefacts from Lübeck. Thanks to M.Sc. H. Hölzig (University Leipzig) for completing XRD measurements and Dr. N. Han (Blacksburg, Virginia, USA) for discussions on the correlation of XRD data with Mg contents of synthetic HMC. Natural coral branches were acquired from Ruppenthal KG (Idar-Oberstein). U. Teschner (University of Leipzig) and A. Flicker (University of Tübingen) carried out Raman spectroscopic measurements. Dr. Jantzen (Schwerin) provided coral beads from Greifs-

wald. For discussions on TEM data of *corallium rubrum* we thank Dr. D. Vielzeuf (Marseille) and for discussions on Raman spectroscopy on polyenes we thank Dr. T. Kupka (Opole). We thank E. Butchereit (Tübingen) for her overall reviewing as well as Dr. J. Ansorge (Greifswald) and M.A. M. Schrickel (Esslingen) for their critical review of the archaeological part of the manuscript. We would also like to thank the Excellence Initiative of the Eberhard Karls University of Tübingen and the Ministry of Science and Research of Baden-Württemberg for funding this work.

References

- Adar, F., 2017. Carotenoids -Their Resonance Raman Spectra and How They Can Be Helpful in Characterizing a Number of Biological Systems. *Electronically reprinted from June 2017 Spectroscopy for materials analyses*.
- Adkins, J.F, Boyle, E.A., Curry, W.B. and Lutringer, A., 2003. Stable isotopes in deep sea corals and a new mechanism for vital effects. *Geochimica et Cosmochimica Acta*, Vol. 67, No. 6, pp.1129-1143.
- Barnard, W. and de Waal, D. 2006. Raman investigation of pigimentary molecules in the molluscan biogenetic matrix. *Journal of Raman Spectroscopy*, 37 (1-3), pp.342-352.
- Bente, K., Berthold, C., Dolz, S. Keuper, M. and Gerdes, A., 2015. Archäometrische Charakterisierung von rotem Schmuckdekor historischer Ethnographica aus dem Königreich Benin (Nigeria), Tunesien und Algerien. In: T. Gluhak, S. Greiff, K. Kraus and M. Prange, eds. 2015. *Archäometrie und Denkmalpflege 2015. Jahrestagung an der Johannes-Gutenberg-Universität Mainz*, 25.-28. März 2015. *Metalla Sonderheft*, 5. Bochum: Deutsches Bergbau-Museum Bochum. pp.129-130.
- Bente, K., Berthold, C., Keuper, M., Gerdes, A., Ansorge, J. and A. König, A., 2017. Die Korallenperlenkette aus Greifswald von um 1300 – archäometrische Untersuchungen an *Corallium rubrum* aus einer mittelalterlichen Hansestadt. The coral pearl necklace from Greifswald from around 1300 – archaeometric investigations on *Corallium rubrum* from a medieval Hanseatic town. *Archäologische Berichte aus Mecklenburg-Vorpommern*, Band 24, pp.69-79.
- Bente, K., Berthold, C., Wirth, R., Schreiber, A., Hölzig, H., Panneerselvam, R.R., Keilholz, S., Poppitz and D., König, A., 2021a. Construction and material signatures of the Przeworst fibula from Leimbach (Nordhausen County, Central Germany). In: S. Greiff, F. Schlütter, A. Kronz and S. Klein, eds. 2021. *Archäometrie und Denkmalpflege 2021. Virtuelle Jahrestagung 17.-19. März 2021*. 25.-28. März 2021. *Metalla Sonderheft*, 11. Bochum: Deutsches Bergbau-Museum Bochum. pp.74-76.
- Bente, K., Gerdes, A., Ende, M., Beirau, T. and Hölzig, H., 2021b. *Provenance signatures of antique coral artefacts by means of Sr-, B-, C- and O-isotopes*. EMC (in press).
- Brückner, W. 1970. Koralle. *Lexikon der christlichen Ikonographie*. Bd. II. Rom, Freiburg, Basel, Wien.
- Chaabane, S., López Correa, M., Montagna, P., Kallel, N., Taviani, M., Linares, C. and Ziveri, P., 2015. Exploring the oxygen and carbon isotopic composition of the Mediterranean red coral (*Corallium rubrum*) for seawater temperature reconstruction. *Marine Chemistry*, 186, pp.11-23.
- Clark, S.J., Jouanna, P., Haines J. and Mainprice, D., 2010. Raman vibration modes of magnesite at high pressure by density-functional perturbation theory and comparison with experiments. *Physics and Chemistry of Minerals*, 38, pp.193-202. <http://dx.doi.org/10.1007/s00269-010-0395-y>.
- Daxelmüller, C., 1982. Heil- und Volksglaube. In: J. Wittstock, ed. 1981. *Kirchliche Kunst des Mittelalters und der Reformationszeit. Lübecker Museumskataloge*, Volume I. Lübeck. pp.181-192.
- Erdmann, W., 1980. Fronerei und Fleischmarkt: Archäologische Befunde eines Platzes im Markviertel des mittelalterlichen Lübeck. In: G.P. Fehring, ed. 1980. *Lübecker Schriften zur Archäologie und Kulturgeschichte*, 3. Bonn: Habelt. pp.107-159.
- Erdmann W., 1985a. Korallenkette aus der Kloake des Lübecker Fronen' um 1400. In: C. Meckseper, ed. 1985. *Stadt im Wandel – Kunst und Kultur des Bürgertums in Norddeutschland 1150-1650*, Bd. 1. Stuttgart. pp.311, Nr. 248.
- Erdmann, W. 1985b. Seidener Gürtel aus der (Kloake des Lübecker Fronen Ende 14. Jahrhundert. In: C. Meckseper, ed. 1985. *Stadt im Wandel, Kunst und Kultur des Bürgertums in Norddeutschland 1150 -1650*, Bd. 1. Stuttgart. pp.311, Nr. 249.
- Erdmann, W. and Nitsch, H., 1986. Spätmittelalterliche und frühneuzeitliche Perlen aus einer Kloake der Fronerei auf dem Schranken zu Lübeck. In: G.P. Fehring, ed. 1986. *Lübecker Schriften zur Archäologie und Kulturgeschichte*, Bd. 12. Bonn: Habelt. pp.137-165.
- Esser, T., 1898. *Zur Archäologie der Pater Noster-Schnur*. Comptendu du quatrième congrès scientifique international des Catholiques à Fribourg (Suisse) 1897. Fribourg. IX. Art Chrétien, Archéologie, Épigrapie.
- Falk, A., 1987. Archäologische Funde und Befunde im späten Mittelalters und der frühen Neuzeit Lübeck. In: A. Falk and R. Hammel, eds 1987. *Archäologische und schriftliche Quellen zur spätmittelalterlich-neuzeitlichen Geschichte der Hansestadt Lübeck. Materialien und Methoden einer archäologisch-historischen Auswertung*. *Lübecker Schriften zur Archäologie und Kulturgeschichte*, 10. Bonn: Habelt. pp.9-84.
- Fan, L., 2018. Precious Coral. In: C. Duque and E.T. Camacho, eds. 2018. *Corals in a changing world*. pp.51-72. <http://dx.doi.org/10.5772/65203>.
- Filip, J., 1969. *Enzyklopädisches Handbuch zur Ur- und Frühgeschichte Europas*. Berlin, Köln, München.
- Floquet, N. and Vielzeuf, D., 2011. Mesoscale twinning and crystallographic registers in biominerals. *American Mineralogist*, 96 (8-9), pp.1228-1237.
- Floquet, N., Vielzeuf, D., Ferry, D., Ricolleau, A., Heresanu, V., Perrin, J., Laporte, D. and Fitch, A.N., 2015. Thermally induced modifications and phase transformations of red coral Mg calcite skeletons from infrared spectroscopy

- and high resolution synchrotron powder diffraction analyses. *Crystal Growth & Design*, 15, pp.4098-4103.
- Fohlmeister, J., Arps, J., Spötl, C., Schröder-Ritzrau, A., Plessen, B., Günter, C., Frank, N. and Trüssel, M., 2018. *Geochimica et Cosmochimica Acta*, 235, pp.127-139.
- Fritsch, E., Rondeau, B., Hainschwang, T. and Karampelas, S., 2009. Raman spectroscopy applied to gemmology. *Elements*, Volume 1, No.3. <https://www.cigem.ca/research/GeoRamanGemmology.pdf>.
- Fritz, J.M., 1982. *Goldschmiedekunst in der Gotik in Mitteleuropa*. München. Pantheon XLI (1983). pp.175-176.
- Fürst, S., 2014. Korallen am Übergang zur Frühlatènezeit. Zum wissenschaftlichen Potenzial eines problematischen Schmuckmaterials. In: S. Hornung, ed. 2014. *Produktion – Distribution – Ökonomie. Siedlungs- und Wirtschaftsmuster der Latènezeit. Akten des internationalen Kolloquiums in Otzenhausen, 28.-30. Oktober 2011. Universitätsforschungen zur prähistorischen Archäologie*, 258. Bonn. pp.41-66.
- Goldsmith, J.R., 1961. Exsolutions of dolomite from calcite. *The Journal of Geology*, 68, pp.103-109.
- Grabner, E. 1969. Die Koralle in Volksmedizin und Aberglauben. *Zeitschrift für Volkskunde*, 65, pp.183-195.
- Grimm, J. and Grimm, W., 1971. *Deutsches Wörterbuch von Jacob und Wilhelm Grimm*. Leipzig 1854-1961. Quellenverzeichnis Leipzig. Online-Version vom 05.03.2020.
- Gunasekaran, S., Anblalagan, G. and Pandi, S., 2006. *Raman and infrared spectra of carbonates of calcite structure*. *Journal of Raman Spectroscopy*, 37, p.892-899.
- Hammel, R., 1987. Hauseigentum im spätmittelalterlichen Lübeck- Methoden sozial- und wirtschaftsgeschichtlicher Auswertung der Lübecker Oberstadtbuch-Regesten. In: A. Falk and R. Hammel, eds. 1987. *Schriftliche Quellen und archäologische Funde zur spätmittelalterlichen und frühneuzeitlichen Stadtgeschichte Lübecks*. *Lübecker Schriften zur Archäologie und Kulturgeschichte*, 10. Bonn: Habelt.
- Han, N., Blue, C.R., De Yoreo, J.J. and Dove, P.M., 2013. The effect of carboxylates on the Mg content of calcites that transform from ACC. *Procedia Earth and Planetary Science*, 7, pp.223-227.
- Hasse, M., 1961. *Die Törichten und die Klugen*. Lübecker Museumshefte, 3. Lübeck.
- Hasse, M., 1981a. Lübecks Kunst im Mittelalter. In: J. Wittstock, ed. 1981. *Kirchliche Kunst des Mittelalters und der Reformationszeit*. *Lübecker Museumskataloge*, Volume I. Lübeck. pp.20-39.
- Hasse, M., 1981b. Neues Hausgerät' neue Häuser, neue Kleider – eine Betrachtung der städtischen Kultur im 13. und 14. Jahrhundert sowie ein Katalog der metallenen Hausgeräte. *Zeitschrift für Archäologie des Mittelalters*, 7, pp.7-83.
- Hauschild, W.D., 1981. *Kirchengeschichte Lübeck. Christentum und Bürgertum in neun Jahrhunderten*. Lübeck.
- Hedegaard, C., Bardeau, J.F. and Chateigner, D., 2006. Molluscan shell pigments: An in situ resonance Raman study. *Journal of Molluscan Studies*, 72(2).
- Herrmann, B., 1986. Parasitologische Untersuchungen eines spätmittelalterlich-frühneuzeitlichen Kloakeninhaltes aus der Fronerei auf dem Schragen in Lübeck. *Lübecker Schriften zur Archäologie und Kulturgeschichte*, 12. Bonn: Habelt. pp.167-172.
- Karampelas, S., Fritsch, E., Mevellec, S., Klavounos, S. and Soldatos, T., 2009. Role of polyenes in the coloration of cultured freshwater pearls. *European Journal of Mineralogy*, 21, pp.85-97.
- Keuper, M., Bente, K., Berthold, C., Wendling, H., Teschner, U. and Münster, T., 2015. Provenance and colour of Latène and Hallstatt period fibulae beads. In: T. Gluhak, S. Greiff, K. Kraus and M. Prange, eds. 2015. *Archäometrie und Denkmalpflege 2015. Jahrestagung an der Johannes-Gutenberg-Universität Mainz, 25.-28. März 2015*. *Metalla Sonderheft*, 5. Bochum: Deutsches Bergbaumuseum Bochum. pp.129-130.
- Kupka, T., Lin, H.M., Stobinski, L., Chen, C.H., Liou, W.J., Wrzalike, R. and Flisak, Z., 2010. Experimental and theoretical studies on corals. I. Toward understanding the origin of color in precious red corals from Raman and IR spectroscopies and DFT calculations. *Journal of Raman Spectroscopy*, 41, pp.651-65.
- Kupka, T., Buczek, A., Broda, M.A., Szosta, R., Lin, H.M., Fan, L.W., Wrzalik, R. and Stobiński, L., 2016a. Modeling red coral (*Corallium rubrum*) and African snail (*Helix aspersa*) shell pigments: Raman spectroscopy vs. DFT studies. *Journal of Raman Spectroscopy*, 47, pp.908-916. <https://doi.org/10.1002/jrs.4922>.
- Kupka, T., Buczek, A., Broda, M., A., Stachow, M. and Tarnowski, P., 2016b. DFT studies on the structural and vibrational properties of polyenes. *Journal of Molecular Modeling*, 22, p.101. <https://doi.org/10.1007/s00894-016-2969-1>.
- Legner, A. ed., 1978. *Die Parler und der Schöne Stil 1350-1400. Europäische Kunst unter den Luxemburgern, ein Handbuch zur Ausstellung*. 3 Bände.
- Mührenberg, D., 1984. *Grabungen auf den Grundstücken Hundestraße in Lübeck: Stratigraphie und Chronologie, Bau- und Besiedlungsgeschichte im Mittelalter*. Master thesis. Universität Hamburg.
- Peelen, J.G.J. and Metselaar, R., 1974. Light scattering by pores in polycrystalline materials: Transmission properties of alumina. *Journal of Applied Physics*, 45, p.216. <https://doi.org/10.1063/1.1662961>.
- Perrin, J., Vielzeuf, D., Ricolleau, A., Dalla Porta, H., Valton, S. and Floquet, N., 2015. Block-by-block and layer-by-layer growth modes in coral skeletons. *American Mineralogist*, Volume 100, pp.681-695.
- Railsback, L.B., 2006. Solubility of common carbonate minerals. Some fundamentals of Mineralogy and Geochemistry. *LBR 820HMC-LMCSolubilities05*, 4/95.
- Ritz, G.M., 1975. Der Rosenkranz. In: Erzbischöfliches Diözesan-Museum Köln, ed. 1975. *500 Jahre Rosenkranz. 1475-1975. Kunst und Frömmigkeit im Spätmittelalter und ihr Weiterleben*. Köln. pp.51-101.
- Schröckel, M. and Bente, K., 2013. Bedeutung und Bedeutungsverlust roter Korallen. Archäologische und naturwissenschaftliche Studien zu eisenzeitlichen Fibeln. In: H. Meller, C.H. Wunderlich and F. Knoll, eds. 2013. *Rot*

– *Die Archäologie bekennt Farbe*. 5 Mitteldeutscher Archäologentag vom 4. bis 6. Oktober 2012 in Halle (Saale). Tagungen des Landesmuseums für Vorgeschichte Halle 10. Halle (Saale): Landesamt für Denkmalpflege und Archäologie (Landesmuseum für Vorgeschichte). pp.341-352.

Schröckel, M., Bente, K., Berthold, C., Grill, W., Teschner, U., Sarge, C. and Hoppe, T., 2014. Vergleichende archäometrische Untersuchungen an Fibeln mit Korallenzier. Fragestellungen und methodischer Überblick. In: S. Hornung, ed. 2014. *Produktion – Distribution – Ökonomie. Siedlungs- und Wirtschaftsmuster der Latènezeit*. Akten internationales Kolloquium Otzenhausen, 28.-30. Oktober 2011.

Schumann, W., 1976. *Edelsteine und Schmucksteine*. - Bestimmungsbuch 17. München, Bern, Wien: BLV Verlagsgesellschaft.

Stephan, H.G., 1978. Archäologische Ausgrabungen im Handwerkerviertel der Hansestadt Lübeck (Hundestraße 9-17) – ein Vorbericht. In: *Lübecker Schriften zur Archäologie und Kulturgeschichte*, 1. Bonn: Habelt. pp.75-80.

Urmos, J., Sharma, S.K., and Mackenzie, F.T., 1971. Characterization of some biogenic carbonates with Raman spectroscopy. *American Mineralogist*, Volume 76, pp.641-646.

Vielzeuf, D. Garrabou, J., Baronet, A., Grauby, O. and Marschal, C., 2008. Nano to macroscale biomineral architecture of red coral (*Corallium rubrum*). *American Mineralogist*, Volume 93, pp.1799-1815.

Volckmann, E., 1921. *Alte Gewerbe und Gewerbegassen. Deutsche Berufs-, Handwerks- und Wirtschaftsgeschichte älterer Zeit*. Würzburg.

Wehrmann, K.F., 1984. *Die älteren lübeckischen Zunftrollen*. Lübeck.

Wittstock, J., 1981. *Kirchliche Kunst des Mittelalters und der Reformationszeit*. Lübecker Museumskataloge, Volume I. Lübeck.

Authors

Klaus Bente (Corresponding author)

CCA-BW Universität Tübingen

Wilhelmstraße 56

D-72074 Tübingen

bente46@gmx.de

Institut für Mineralogie, Kristallographie und

Materialwissenschaft, Universität Leipzig

Scharnhorststr. 20

04275 Leipzig

bente@rz.uni-leipzig.de

Christoph Berthold

CCA-BW Universität Tübingen

Wilhelmstraße 56, D-72074 Tübingen

Christoph.Berthold@uni-tuebingen.de

Richard Wirth

GFZ Potsdam Section 3.5 Surface Geochemistry

Telegrafenberg

14473 Potsdam

richard.wirth@gfz-potsdam.de

Anja Schreiber

GFZ Potsdam Section 3.5 Surface Geochemistry

Telegrafenberg

14473 Potsdam

aschreib@gfz-potsdam.de

Andreas König

Poliklinik für Zahnärztliche Prothetik und

Werkstoffkunde, Universität Leipzig

Liebigstraße 12

04103 Leipzig

andreas.koenig@medizin.uni-leipzig.de